



# Over 20% $^{15}\text{N}$ Hyperpolarization in Under One Minute for Metronidazole, an Antibiotic and Hypoxia Probe

Danila A. Barskiy,<sup>†,#</sup> Roman V. Shchepin,<sup>†,#</sup> Aaron M. Coffey,<sup>†</sup> Thomas Theis,<sup>‡</sup> Warren S. Warren,<sup>‡</sup> Boyd M. Goodson,<sup>§</sup> and Eduard Y. Chekmenev<sup>\*,†,||,⊥</sup>

<sup>†</sup>Department of Radiology, Vanderbilt University Institute of Imaging Science, Vanderbilt University Medical Center, Nashville, Tennessee 37232, United States

<sup>‡</sup>Department of Chemistry, Duke University, Durham, North Carolina 27708, United States

<sup>§</sup>Department of Chemistry and Biochemistry and Materials Technology Center, Southern Illinois University, Carbondale, Illinois 62901, United States

<sup>||</sup>Department of Biomedical Engineering, Vanderbilt-Ingram Cancer Center, Vanderbilt University, Nashville, Tennessee 37232, United States

<sup>⊥</sup>Russian Academy of Sciences, Leninskiy Prospekt 14, Moscow 119991, Russia

## S Supporting Information

**ABSTRACT:** Direct NMR hyperpolarization of naturally abundant  $^{15}\text{N}$  sites in metronidazole is demonstrated using SABRE-SHEATH (Signal Amplification by Reversible Exchange in SHield Enables Alignment Transfer to Heteronuclei). In only a few tens of seconds, nuclear spin polarization  $P^{15\text{N}}$  of up to  $\sim 24\%$  is achieved using parahydrogen with 80% *para* fraction corresponding to  $P^{15\text{N}} \approx 32\%$  if  $\sim 100\%$  parahydrogen were employed (which would translate to a signal enhancement of  $\sim 0.1$ -million-fold at 9.4 T). In addition to this demonstration on the directly binding  $^{15}\text{N}$  site (using  $J_{\text{H-}^{15}\text{N}}^2$ ), we also hyperpolarized more distant  $^{15}\text{N}$  sites in metronidazole using longer-range spin–spin couplings ( $J_{\text{H-}^{15}\text{N}}^4$  and  $J_{\text{H-}^{15}\text{N}}^5$ ). Taken together, these results significantly expand the range of molecular structures and sites amenable to hyperpolarization via low-cost parahydrogen-based methods. In particular, hyperpolarized nitroimidazole and its derivatives have powerful potential applications such as direct *in vivo* imaging of mechanisms of action or hypoxia sensing.

NMR hyperpolarization techniques increase nuclear spin polarization from thermal equilibrium levels of  $10^{-6}$ – $10^{-5}$  by orders of magnitude—in some cases approaching 100%.<sup>1–4</sup> Adequately chosen nuclear spin sites can retain their hyperpolarized (HP) state for many minutes, decaying exponentially back to thermal equilibrium; when this decay is slow enough, HP substances can be used as exogenous contrast agents to probe metabolism and function *in vivo*.<sup>2,5,6</sup>  $^{15}\text{N}$  sites are particularly interesting because of their greater (e.g., compared to  $^{13}\text{C}$ ) decay constants of up to 20 min.<sup>7–10</sup> Moreover,  $^{15}\text{N}$  isotopic enrichment is frequently performed using relatively straightforward and efficient chemistries and therefore could be significantly more cost-effective than production of  $^{13}\text{C}$ -enriched compounds such as  $1\text{-}^{13}\text{C}$ -pyruvate.<sup>11,12</sup> Currently, the rapidly growing field of HP  $^{13}\text{C}$  molecular contrast agents is dominated by dissolution Dynamic Nuclear Polarization (d-DNP), which typically achieves  $^{13}\text{C}$

polarization levels well above 10%.<sup>13</sup> However, for hyperpolarization of  $^{15}\text{N}$  sites, the efficiency of d-DNP has been limited to a few percent and currently requires hours of polarization time. To date,  $^{15}\text{N}$ -choline ( $P^{15\text{N}} \approx 3\%$  in 2.5 h),<sup>14</sup> pH sensors ( $P^{15\text{N}} \leq 3\%$  in 2 h),<sup>15</sup> and a calcium sensor ( $P^{15\text{N}} < 2\%$ )<sup>16</sup> have been polarized by d-DNP for potential use as injectable HP contrast agents.

Direct hyperpolarization of heteronuclei with NMR Signal Amplification by Reversible Exchange (SABRE<sup>17</sup>) is possible via SABRE-SHEATH (SABRE in SHield Enables Alignment Transfer to Heteronuclei).<sup>18,19</sup> Unlike d-DNP, SABRE-SHEATH<sup>18,19</sup> is scalable, provides efficient hyperpolarization in seconds, and uses very simple and inexpensive hardware.<sup>7,20</sup>  $^{15}\text{N}$  SABRE-SHEATH of several biomolecules has been demonstrated (including nicotinamide,<sup>11,18</sup> imidazole,<sup>21</sup> and diazirines<sup>7</sup>), producing  $P^{15\text{N}}$  of up to 10% in  $\leq 1$  min. It is our goal to expand the range of biomedically useful compounds amenable to SABRE-SHEATH, which may enable unprecedented molecular imaging and spectroscopy experiments that would provide direct visualization of biochemical processes.

Despite the success of  $^{15}\text{N}$  SABRE-SHEATH, so far this new approach has been limited to hyperpolarization of  $^{15}\text{N}$  sites directly binding to the polarization-transfer catalyst. This pathway exploits short-range two-bond spin–spin couplings ( $J_{\text{H-}^{15}\text{N}}^2$ ) for polarization transfer from parahydrogen to  $^{15}\text{N}$  sites (Figure 1a) in a  $\mu\text{T}$  magnetic field ( $B_T$ ).<sup>18,19</sup> Furthermore, sterically hindering groups (e.g., methyl groups) in the ortho-positions of six-membered N-heterocycles significantly reduce the efficiency of polarization transfer.<sup>22</sup> These shortcomings limit the use of  $^{15}\text{N}$ -SABRE-SHEATH.

Here we overcome these limitations and demonstrate  $^{15}\text{N}$  SABRE-SHEATH on metronidazole, a member of an important group of antibiotics—the nitroimidazoles. Nitroimidazoles were discovered in the 1950s as a class of antibiotics acting on a wide range of anaerobic bacterial infections.<sup>23</sup>

Received: May 9, 2016

Published: June 20, 2016



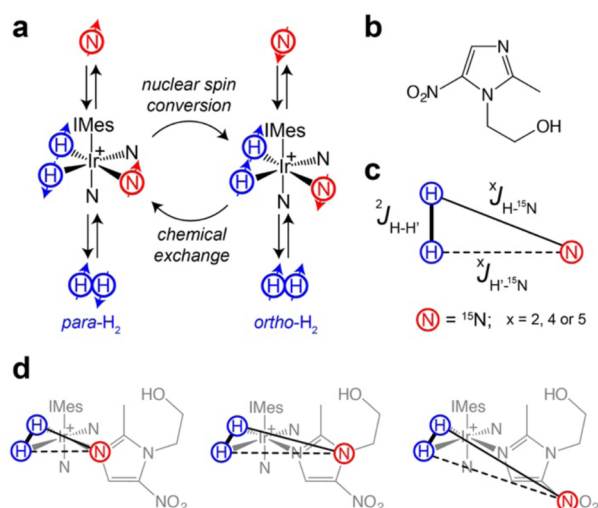


**Figure 1.** (a) Schematic diagram of the SABRE process: coherent polarization transfer from parahydrogen-derived hydrides to  $^{15}\text{N}$  heteronuclei. (b) Molecular structure of metronidazole. (c) Schematic representation of the AA'B spin system in the polarization transfer complex. Red circles represent naturally abundant  $^{15}\text{N}$  nuclei. (d) Most-probable metronidazole-bound structures of the complex with relevant AA'B spin systems.

Anaerobic conditions protect the organism's employment of pyruvate synthase, which consequently acts irreversibly on the nitroimidazole moiety—leading to selective drug uptake by anaerobic bacterial cells in the host.<sup>23</sup> The sensitivity of nitroimidazole moieties to anaerobic conditions was later exploited for hypoxia sensing in cancer. Despite a different mechanism of action<sup>23</sup> in mammalian anaerobic cancer cells, the end result is the same: the chemical reaction of the nitro moiety leads to irreversible binding in hypoxic cells.<sup>24,25</sup> A number of nitroimidazole compounds were employed as molecular contrast agents to probe hypoxia and upregulation of hypoxia inducible factor (HIF-1 $\alpha$ ) using Positron Emission Tomography (PET),<sup>26</sup> and Magnetic Resonance (MR) imaging and spectroscopy.<sup>27</sup> Hypoxia is a hallmark of some aggressive forms of cancer,<sup>28,29</sup> and its imaging can be used as a biomarker for cancer screening and monitoring response to treatment.<sup>26,30</sup> The investigational use of fluoromisonidazole (FMISO),<sup>26</sup> SR4554,<sup>27</sup> and numerous other related nitroimidazole-based agents for hypoxia imaging has advanced well into clinical trials. Furthermore, the intravenous injection of up to 1.4 g/m<sup>2</sup> of nitroimidazole derivatives is well tolerated in patients,<sup>27</sup> which would certainly be sufficient for HP imaging.<sup>31</sup>

In the present SABRE-SHEATH hyperpolarization studies, we employed the most efficient IrIMes polarization-transfer catalyst (using the established Ir catalyst precursor [IrCl(COD)(IMes)]; IMes = 1,3-bis(2,4,6-trimethylphenyl)imidazol-2-ylidene; COD = cyclooctadiene)<sup>32,33</sup> and metronidazole with  $^{15}\text{N}$  at natural abundance ( $\sim 0.364\%$ ). As this abundance is low, the statistically most-abundant polarization-transfer species contains only one  $^{15}\text{N}$  site. Therefore, the relevant spin system for polarization transfer contains only three spins: two magnetically inequivalent protons and one  $^{15}\text{N}$  site (Figure 1c).<sup>22,34</sup> Because metronidazole contains three nitrogen sites, it can form three types of AA'B spin systems, respectively involving two-bond, four-bond, or five-bond spin-spin couplings (Figure 1d). The  $^{15}\text{N}$  NMR signal from nitrogens only two bonds away from the nascent parahydrogen

pair was enhanced by  $\sim 72\,000$ -fold at 9.4 T (corresponding to  $P_{^{15}\text{N}} \approx 24\%$ ; see Supporting Information (SI) for additional experimental and analysis details) in 50 mM solution of metronidazole in methanol- $d_4$  using  $\sim 80\%$  parahydrogen (Figure 2b); these results may be extrapolated to expect  $P_{^{15}\text{N}}$

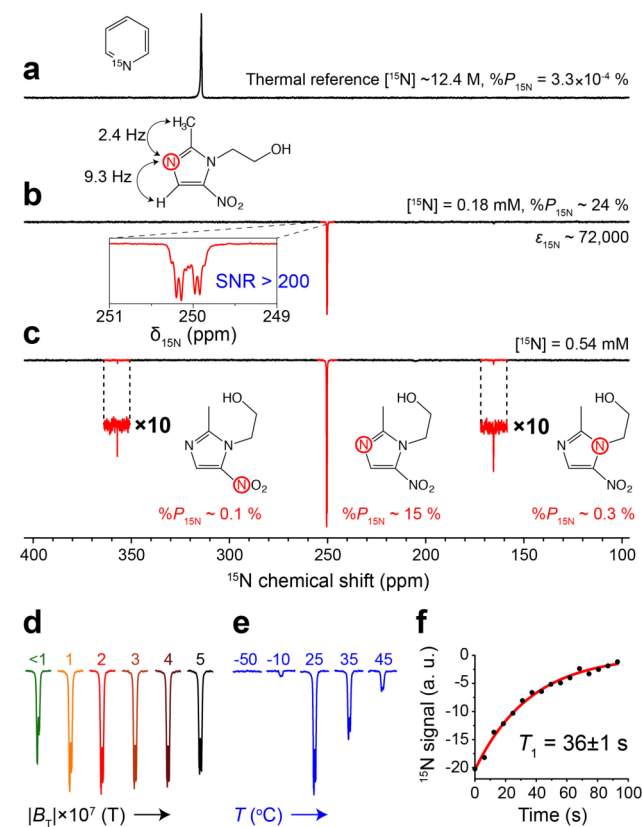


**Figure 2.** (a)  $^{15}\text{N}$  NMR spectrum of thermally polarized signal reference, neat pyridine- $^{15}\text{N}$  ( $\sim 12.4$  M). (b)  $^{15}\text{N}$  spectrum of HP natural abundance 50 mM metronidazole at  $\sim 298$  K. Note the appearance of NMR resonances as a doublet of quartets due to spin-spin coupling of  $^{15}\text{N}$  with aromatic and methyl protons (inset). (c)  $^{15}\text{N}$  spectrum of HP natural abundance 150 mM metronidazole at  $\sim 298$  K. (d) Optimization of HP metronidazole  $^{15}\text{N}$  NMR signal by varying the magnetic field in the shield ( $B_1$ ). (e) Optimization of HP metronidazole  $^{15}\text{N}$  NMR signal by varying the temperature (estimated values) of the sample. (f)  $^{15}\text{N}$   $T_1$  signal decay of HP metronidazole in methanol- $d_4$  at 9.4 T. All HP  $^{15}\text{N}$  spectra shown were obtained using 80% parahydrogen gas.

$\approx 32\%$  if  $\sim 100\%$  parahydrogen were employed. Note that the  $^{15}\text{N}$  polarization was sampled  $\sim 8$  s after cessation of parahydrogen bubbling, and the measurement does not take into account polarization decay losses that have occurred during the sample transfer from the hyperpolarization setup into the bore of the 9.4 T NMR spectrometer. The  $P_{^{15}\text{N}}$  value of  $\sim 24\%$  is the highest  $^{15}\text{N}$  hyperpolarization level achieved by any technique to date by at least several-fold, and it is demonstrated despite the presence of one or two ortho substituents, which have previously prevented the observation of SABRE-SHEATH enhancement of six-membered N-heterocycles.<sup>22</sup> This high level of  $P_{^{15}\text{N}}$  is not far away from the practical limit of 50% theoretically predicted in recent literature.<sup>34–36</sup> Furthermore, investigations using more concentrated solutions ( $\sim 150$  mM, Figure 2c, and  $\sim 100$  mM, Figure S5) additionally enabled detection of relatively efficient SABRE-SHEATH

hyperpolarization of the other two  $^{15}\text{N}$  sites (more weakly coupled, via  $J_{\text{H-}^{15}\text{N}}^4$  and  $J_{\text{H-}^{15}\text{N}}^5$  couplings). Although these other two sites exhibited significantly more modest  $P^{15}\text{N}$  values of 0.1–0.3% (i.e., “only” ~1000-fold enhancements), it should be noted that neither the  $\mu\text{T}$  field nor the exchange rates governing the SABRE-SHEATH process were optimized for hyperpolarization of these two remote  $^{15}\text{N}$  sites. The feasibility of  $^{15}\text{N}$  SABRE-SHEATH processes via long-range (up to  $J_{\text{H-}^{15}\text{N}}^5$ ) spin–spin couplings (in a manner similar to homonuclear SABRE<sup>17,32,37</sup>) enables  $^{15}\text{N}$  hyperpolarization of a wider range of biomolecules via SABRE-SHEATH, because more  $^{15}\text{N}$  and potentially other heteronuclear sites become amenable to SABRE-SHEATH.

It should also be emphasized that  $^{15}\text{N}$  NMR spectra with high signal-to-noise ratios (SNRs >200 and >100) were recorded despite the low natural abundance of  $^{15}\text{N}$  and despite using only 80% parahydrogen (Figure 2) and 50% parahydrogen (see SI spectra), respectively. Moreover, this SNR level is more than sufficient for optimization of experimental conditions, i.e., the  $\mu\text{T}$  magnetic field for polarization transfer  $B_{\text{T}}$ , temperature, and measurements of relaxation parameters (see Figure 2d–f). Furthermore, the reported  $^{15}\text{N}$   $T_1$  ( $36 \pm 1$  s) relaxation is dominated by  $^{15}\text{N}$  Chemical Shift Anisotropy (CSA) at high magnetic field (e.g., 9.4 T used here), and  $T_1$  is significantly extended (by several-fold) at the clinically relevant fields of 1.5 T and below.<sup>7</sup> An expected *in vivo*  $^{15}\text{N}$   $T_1$  of 1–2 min<sup>14</sup> may be sufficient for hypoxia sensing, because nitroimidazole-based compounds reach the hypoxic region within the first minute after intravenous injection.<sup>38,39</sup> Moreover, while other tissues may also absorb the injected hypoxia sensor,<sup>27,38,39</sup> the  $^{15}\text{N}$  chemical shifts of the reduced form of the nitroimidazole moiety may be sufficiently different to provide a good mechanism of contrast of hypoxic regions versus surrounding tissues—mitigating the requirement for clearance of the background signal (the subject of future work).

In conclusion, record-level  $^{15}\text{N}$  hyperpolarization was achieved via SABRE-SHEATH in seconds for a representative compound from the nitroimidazole class of antibiotics/contrast agents. Substituted five-membered N-heterocycles can be efficiently hyperpolarized via SABRE-SHEATH even in the presence of ortho substituents.  $^{15}\text{N}$  SABRE-SHEATH of distant nitrogen sites via long-range spin–spin couplings is demonstrated. Moreover, high levels of  $P^{15}\text{N}$  enable detection of HP  $^{15}\text{N}$  compounds even at natural abundance and 50% parahydrogen (see SI for additional  $^{15}\text{N}$  spectra), which can be conveniently utilized for screening of large libraries of compounds. Finally, the advances presented here will likely be synergistically compatible with recent developments of heterogeneous SABRE<sup>40,41</sup> and SABRE in aqueous media,<sup>20,42–45</sup> key elements for future biomedical translation of this work into animal models and ultimately clinical trials.

## ■ ASSOCIATED CONTENT

### Supporting Information

The Supporting Information is available free of charge on the ACS Publications website at DOI: 10.1021/jacs.6b04784.

Additional experimental details, table of calculated values, and NMR spectra in Figures S1–S5 (PDF)

## ■ AUTHOR INFORMATION

### Corresponding Author

\*eduard.chekmenev@vanderbilt.edu

## Author Contributions

#D.A.B. and R.V.S. contributed equally.

## Notes

The authors declare no competing financial interest.

## ■ ACKNOWLEDGMENTS

This work was supported by NSF under grants CHE-1058727, CHE-1363008, CHE-1416268, and CHE-1416432; NIH under T32EB001628, 1R21EB018014, and 1R21EB020323; DOD CDMRP BRP W81XWH-12-1-0159/BC112431; DOD PRMRP awards W81XWH-15-1-0271 and W81XWH-15-1-0272; and ExxonMobil Research and Engineering Company Knowledge Build. We thank Dr. Fan Shi for assistance with the SABRE catalyst.

## ■ REFERENCES

- (1) Nikolaou, P.; Goodson, B. M.; Chekmenev, E. Y. *Chem. - Eur. J.* **2015**, *21*, 3156.
- (2) Kurhanewicz, J.; Vigneron, D. B.; Brindle, K.; Chekmenev, E. Y.; Comment, A.; Cunningham, C. H.; DeBerardinis, R. J.; Green, G. G.; Leach, M. O.; Rajan, S. S.; Rizi, R. R.; Ross, B. D.; Warren, W. S.; Malloy, C. R. *Neoplasia* **2011**, *13*, 81.
- (3) Bowers, C. R.; Weitekamp, D. P. *Phys. Rev. Lett.* **1986**, *57*, 2645.
- (4) Mewis, R. E. *Magn. Reson. Chem.* **2015**, *53*, 789.
- (5) Brindle, K. M. *J. Am. Chem. Soc.* **2015**, *137*, 6418.
- (6) Golman, K.; in't Zandt, R.; Thaning, M. *Proc. Natl. Acad. Sci. U. S. A.* **2006**, *103*, 11270.
- (7) Theis, T.; Ortiz, G. X.; Logan, A. W. J.; Claytor, K. E.; Feng, Y.; Huhn, W. P.; Blum, V.; Malcolmson, S. J.; Chekmenev, E. Y.; Wang, Q.; Warren, W. S. *Sci. Adv.* **2016**, *2*, e1501438.
- (8) Nonaka, H.; Hata, R.; Doura, T.; Nishihara, T.; Kumagai, K.; Akakabe, M.; Tsuda, M.; Ichikawa, K.; Sando, S. *Nat. Commun.* **2013**, *4*, 2411.
- (9) Gabellieri, C.; Reynolds, S.; Lavie, A.; Payne, G. S.; Leach, M. O.; Eykyn, T. R. *J. Am. Chem. Soc.* **2008**, *130*, 4598.
- (10) Pileio, G.; Carravetta, M.; Hughes, E.; Levitt, M. H. *J. Am. Chem. Soc.* **2008**, *130*, 12582.
- (11) Shchepin, R. V.; Barskiy, D. A.; Mikhaylov, D. M.; Chekmenev, E. Y. *Bioconjugate Chem.* **2016**, *27*, 878.
- (12) Oppenheimer, N. J.; Matsunaga, T. O.; Kam, B. L. *J. Labelled Compd. Radiopharm.* **1978**, *15*, 191.
- (13) Ardenkjaer-Larsen, J. H.; Fridlund, B.; Gram, A.; Hansson, G.; Hansson, L.; Lerche, M. H.; Servin, R.; Thaning, M.; Golman, K. *Proc. Natl. Acad. Sci. U. S. A.* **2003**, *100*, 10158.
- (14) Cudalbu, C.; Comment, A.; Kurdzesau, F.; van Heeswijk, R. B.; Uffmann, K.; Jannin, S.; Denisov, V.; Kirik, D.; Gruetter, R. *Phys. Chem. Chem. Phys.* **2010**, *12*, 5818.
- (15) Jiang, W.; Lumata, L.; Chen, W.; Zhang, S.; Kovacs, Z.; Sherry, A. D.; Khemtong, C. *Sci. Rep.* **2015**, *5*, 9104.
- (16) Hata, R.; Nonaka, H.; Takakusagi, Y.; Ichikawa, K.; Sando, S. *Chem. Commun.* **2015**, *51*, 12290.
- (17) Adams, R. W.; Aguilar, J. A.; Atkinson, K. D.; Cowley, M. J.; Elliott, P. I. P.; Duckett, S. B.; Green, G. G. R.; Khazal, I. G.; Lopez-Serrano, J.; Williamson, D. C. *Science* **2009**, *323*, 1708.
- (18) Theis, T.; Truong, M. L.; Coffey, A. M.; Shchepin, R. V.; Waddell, K. W.; Shi, F.; Goodson, B. M.; Warren, W. S.; Chekmenev, E. Y. *J. Am. Chem. Soc.* **2015**, *137*, 1404.
- (19) Truong, M. L.; Theis, T.; Coffey, A. M.; Shchepin, R. V.; Waddell, K. W.; Shi, F.; Goodson, B. M.; Warren, W. S.; Chekmenev, E. Y. *J. Phys. Chem. C* **2015**, *119*, 8786.
- (20) Truong, M. L.; Shi, F.; He, P.; Yuan, B.; Plunkett, K. N.; Coffey, A. M.; Shchepin, R. V.; Barskiy, D. A.; Kovtunov, K. V.; Koptuyug, I. V.; Waddell, K. W.; Goodson, B. M.; Chekmenev, E. Y. *J. Phys. Chem. B* **2014**, *118*, 13882.
- (21) Shchepin, R. V.; Barskiy, D. A.; Coffey, A. M.; Theis, T.; Shi, F.; Warren, W. S.; Goodson, B. M.; Chekmenev, E. Y. *ACS Sensors* **2016**, DOI: 10.1021/acssensors.6b00231.

- (22) Shchepin, R. V.; Truong, M. L.; Theis, T.; Coffey, A. M.; Shi, F.; Waddell, K. W.; Warren, W. S.; Goodson, B. M.; Chekmenev, E. Y. *J. Phys. Chem. Lett.* **2015**, *6*, 1961.
- (23) Upcroft, P.; Upcroft, J. A. *Clin. Microbiol. Rev.* **2001**, *14*, 150.
- (24) Kizaka-Kondoh, S.; Konse-Nagasawa, H. *Cancer Sci.* **2009**, *100*, 1366.
- (25) Masaki, Y.; Shimizu, Y.; Yoshioka, T.; Tanaka, Y.; Nishijima, K.; Zhao, S.; Higashino, K.; Sakamoto, S.; Numata, Y.; Yamaguchi, Y.; Tamaki, N.; Kuge, Y. *Sci. Rep.* **2015**, *5*, 16802.
- (26) Hendrickson, K.; Phillips, M.; Smith, W.; Peterson, L.; Krohn, K.; Rajendran, J. *Radiother. Oncol.* **2011**, *101*, 369.
- (27) Lee, C. P.; Payne, G. S.; Oregioni, A.; Ruddle, R.; Tan, S.; Raynaud, F. I.; Eaton, D.; Campbell, M. J.; Cross, K.; Halbert, G.; Tracy, M.; McNamara, J.; Seddon, B.; Leach, M. O.; Workman, P.; Judson, I. *Br. J. Cancer* **2009**, *101*, 1860.
- (28) Hanahan, D.; Weinberg, R. A. *Cell* **2011**, *144*, 646.
- (29) Gillies, R. J.; Verduzco, D.; Gatenby, R. A. *Nat. Rev. Cancer* **2012**, *12*, 487.
- (30) Evans, S. M.; Jenkins, W. T.; Joiner, B.; Lord, E. M.; Koch, C. J. *Cancer Res.* **1996**, *56*, 405.
- (31) Nelson, S. J.; Kurhanewicz, J.; Vigneron, D. B.; Larson, P. E. Z.; Harzstark, A. L.; Ferrone, M.; van Criekinge, M.; Chang, J. W.; Bok, R.; Park, I.; Reed, G.; Carvajal, L.; Small, E. J.; Munster, P.; Weinberg, V. K.; Ardenkjaer-Larsen, J. H.; Chen, A. P.; Hurd, R. E.; Odegardstuen, L. I.; Robb, F. J.; Tropp, J.; Murray, J. A. *Sci. Transl. Med.* **2013**, *5*, 198ra108.
- (32) Cowley, M. J.; Adams, R. W.; Atkinson, K. D.; Cockett, M. C. R.; Duckett, S. B.; Green, G. G. R.; Lohman, J. A. B.; Kerssebaum, R.; Kilgour, D.; Mewis, R. E. *J. Am. Chem. Soc.* **2011**, *133*, 6134.
- (33) Appleby, K. M.; Mewis, R. E.; Oлару, A. M.; Green, G. G. R.; Fairlamb, I. J. S.; Duckett, S. B. *Chem. Sci.* **2015**, *6*, 3981.
- (34) Barskiy, D. A.; Pravdivtsev, A. N.; Ivanov, K. L.; Kovtunov, K. V.; Koptuyug, I. V. *Phys. Chem. Chem. Phys.* **2016**, *18*, 89.
- (35) Levitt, M. H. *J. Magn. Reson.* **2016**, *262*, 91.
- (36) Knecht, S.; Pravdivtsev, A. N.; Hovener, J.-B.; Yurkovskaya, A. V.; Ivanov, K. L. *RSC Adv.* **2016**, *6*, 24470.
- (37) Eshuis, N.; Aspers, R. L. E. G.; van Weerdenburg, B. J. A.; Feiters, M. C.; Rutjes, F. P. J. T.; Wijmenga, S. S.; Tessari, M. J. *Magn. Reson.* **2016**, *265*, 59.
- (38) Komar, G.; Seppänen, M.; Eskola, O.; Lindholm, P.; Grönroos, T. J.; Forsback, S.; Sipilä, H.; Evans, S. M.; Solin, O.; Minn, H. *J. Nucl. Med.* **2008**, *49*, 1944.
- (39) Shi, K.; Souvatzoglou, M.; Astner, S. T.; Vaupel, P.; Nüsslin, F.; Wilkens, J. J.; Ziegler, S. I. *J. Nucl. Med.* **2010**, *51*, 1386.
- (40) Shi, F.; Coffey, A. M.; Waddell, K. W.; Chekmenev, E. Y.; Goodson, B. M. *Angew. Chem., Int. Ed.* **2014**, *53*, 7495.
- (41) Shi, F.; Coffey, A. M.; Waddell, K. W.; Chekmenev, E. Y.; Goodson, B. M. *J. Phys. Chem. C* **2015**, *119*, 7525.
- (42) Hövener, J.-B.; Schwaderlapp, N.; Borowiak, R.; Lickert, T.; Duckett, S. B.; Mewis, R. E.; Adams, R. W.; Burns, M. J.; Highton, L. A. R.; Green, G. G. R.; Oлару, A.; Hennig, J.; von Elverfeldt, D. *Anal. Chem.* **2014**, *86*, 1767.
- (43) Zeng, H.; Xu, J.; McMahon, M. T.; Lohman, J. A. B.; van Zijl, P. C. M. *J. Magn. Reson.* **2014**, *246*, 119.
- (44) Shi, F.; He, P.; Best, Q. A.; Groome, K.; Truong, M. L.; Coffey, A. M.; Zimay, G.; Shchepin, R. V.; Waddell, K. W.; Chekmenev, E. Y.; Goodson, B. M. *J. Phys. Chem. C* **2016**, *120*, 12149.
- (45) Spannring, P.; Reile, I.; Emondts, M.; Schleker, P. P. M.; Hermkens, N. K. J.; van der Zwaluw, N. G. J.; van Weerdenburg, B. J. A.; Tinnemans, P.; Tessari, M.; Blümich, B.; Rutjes, F. P. J. T.; Feiters, M. C. *Chem. - Eur. J.* **2016**, DOI: 10.1002/chem.201601211.